S-model calculations for high-energy-electron-impact double ionization of helium

G. Gasaneo,[1,*] D. M. Mitnik,[2,*] J. M. Randazzo,[3,*] L. U. Ancarani,[4] and F. D. Colavecchia[3,*]

[1]*Departamento de Física, Universidad Nacional del Sur, 8000 Bahía Blanca, Buenos Aires, Argentina*

[2]*Instituto de Astronomía y Física del Espacio, FCEyN Universidad de Buenos Aires, Argentina*

[3]*División Física Atómica, Molecular y Óptica, Centro Atómico Bariloche and 8400 S. C. de Bariloche, Río Negro, Argentina*

[4]*Théorie, Modélisation, Simulation, SRSMC, UMR CNRS 7565, Université de Lorraine, 57078 Metz, France*

(Received 12 December 2012; published 29 April 2013)

In this paper the double ionization of helium by high-energy electron impact is studied. The corresponding four-body Schrödinger equation is transformed into a set of driven equations containing successive orders in the projectile-target interaction. The transition amplitude obtained from the asymptotic limit of the first-order solution is shown to be equivalent to the familiar first Born approximation. The first-order driven equation is solved within a generalized Sturmian approach for an S-wave $(e,3e)$ model process with high incident energy and small momentum transfer corresponding to published measurements. Two independent numerical implementations, one using spherical and the other hyperspherical coordinates, yield mutual agreement. From our *ab initio* solution, the transition amplitude is extracted, and single differential cross sections are calculated and could be taken as benchmark values to test other numerical methods in a previously unexplored energy domain.

DOI: 10.1103/PhysRevA.87.042707 PACS number(s): 34.80.Dp, 34.50.−s

I. INTRODUCTION

The study of electron-impact double ionization of atoms allows one to learn about correlated systems. The most detailed information is obtained through a kinematically complete $(e,3e)$ experiment, in which the three outgoing particles are detected in coincidence and a fivefold differential cross section (FDCS) is deduced. At high impact energy, the only available absolute experimental $(e,3e)$ data for helium have been published by the Orsay group [1,2]. The coplanar measurements were performed with an incoming projectile of 5600 eV, two different sets of ejected electrons energies ($4+4$ eV and $10+10$ eV), and a small scattering angle corresponding to small momentum transfers $q = 0.22$ a.u. and $q = 0.24$ a.u.: the conditions are such that the first Born approximation should be suitable. In spite of this, no theoretical study has yet managed to describe satisfactorily all the data. What is more confusing, and difficult to explain, is that several *ab initio* methods provide different answers both in FDCS shapes and magnitudes (see a review in Ref. [3]). The main aim of this paper is not to attempt to resolve the situation, but rather to provide—for these high projectile energies—benchmark cross sections which, hopefully, other *ab initio* methods will reproduce. If agreement can be found, at least for the simplified e^--He S-wave $(e,3e)$ model proposed below, then one can start exploring more deeply the reasons beyond the above-mentioned disagreements for the real problem.

From a theoretical point of view, the description of an $(e,3e)$ process on helium requires the solution of a pure four-body Coulomb problem. However, a reduction to a three-body problem can be performed in the case of high-energy projectiles as those used in the Orsay experiment. For two electrons escaping with energies E_2 and E_3 in the solid angles $d\Omega_2$ and $d\Omega_3$, the FDCS—within the first Born approximation—is defined as [4]

$$\frac{d^5\sigma}{d\Omega_2 d\Omega_3 d\Omega_f dE_2 dE_3} = (2\pi)^4 \frac{k_f k_2 k_3}{k_i} |T_{fi}|^2, \tag{1}$$

in terms of the transition matrix

$$T_{fi} = \frac{4\pi}{q^2} \langle \Psi_f^- | W | \Psi_0 \rangle. \tag{2}$$

Here $\mathbf{q} = \mathbf{k}_i - \mathbf{k}_f$ is the momentum transferred to the target [projectile with initial ($\mathbf{k}_i$) and final ($\mathbf{k}_f$) momenta], and W contains the Fourier transform of the interaction between the projectile and the three target particles. Only three-body wave functions are required in (2): Ψ_0 representing the helium ground state, and a double continuum Ψ_f^- describing the movement of the two ejected electrons (momenta k_2 and k_3) in the presence of the residual target ion.

Various methods have been developed in the past decades to describe both types of three-body states. The description of the double continuum is by far the most difficult both from the theoretical as well as the numerical point of view, the main difficulty being the imposition of appropriate asymptotic behaviors. *Ab initio* methods like the R matrix [5], J matrix [6,7], convergent close coupling [8], and exterior complex scaling [9] have been very successful in describing the single ionization of atoms by electron impact. For the simplest case, the ionization of hydrogen by electron impact, really good agreement has been found not only between several *ab initio* methods but also in their comparison with the available experimental data. This very satisfactory picture suggests that all the methods provide an appropriate description of the double continuum of a three-body Coulomb system (or at least they numerically manage to find convergence towards the exact solution of the problem). From these observations, it can be stated that the three-body scattering problem has been solved *numerically*. This idyllic situation, however, is not encountered when applying the same double continuum wave function to describe $(e,3e)$ processes within the first Born approximation. When comparing the results provided by

[*]Also at Consejo Nacional de Investigaciones Científicas y Técnicas, CONICET, Argentina.

ab initio methods, no concluding agreement is found with the two sets of absolute experimental data. What is even more significant, and unsatisfactory from a theoretical point of view, is that no agreement is found between the different *ab initio* methods [3]. This is difficult to understand (and accept) because they should all provide the exact solutions of the three-body problem.

The full solution of the four-body Coulomb problem within the context of collisional processes requires a huge amount of computational resources. In particular, the triple continuum scattering wave function necessary to study a $(e,3e)$ process has been obtained only within a time-dependent treatment which, however, is restricted, again by computational limitations, to low energies of the projectile and of the ejected electrons [10,11]. A time-dependent treatment with the high impact energy of the Orsay experiment has also been implemented using a wave-packet evolution combined with the exterior complex scaling technique [12]. Even when the shapes of the cross sections obtained are in relatively good agreement with the different data sets, this method presents a disagreement in magnitude being, on average, of a factor 2.6 when compared with the 10 eV data, and a factor 8.5 when compared with the 4 eV set. Two other *ab initio* treatments of the process have been implemented, namely the convergent-close-coupling [13] and the *J*-matrix approaches [6,7,14]. The close-coupling approach has a more or less good representation of the FDCS angular shapes, but fails by magnitude factors of 3.2 (respectively 14) with the 10 eV (respectively 4 eV) data sets. The *J*-matrix approach [6,7] also presents a disagreement in magnitude when compared with the other methods and with the experimental data [3]. Very recently, the group of Piraux implemented a *J*-matrix approach [14] and found a reasonable overall agreement with both sets of experimental data; however, due to convergence problems that appear in the formulation, the authors stated that their results cannot be considered as conclusive. Thus, overall, the situation is far from being resolved.

In order to contribute in elucidating this confusing picture, we propose here to study an e^--He double-ionization *S*-wave model, providing data which could be used to test numerical methods. To describe $(e,3e)$ processes, we first introduce a high-energy approach where convergence problems are avoided; the formulation, based on the expansion of the wave function in powers of the projectile interactions, is equivalent to the Born series but written in terms of driven differential equations. The solution to the zero- and first-order equations contains the first Born approximation for the full four-body problem. The advantage of our proposal is that it leads to a three-body problem where no convergency problems arise since the driven term contains the helium ground state and is therefore of short range. Within this formalism, we propose to study a helium double-ionization *S*-wave model. We shall solve numerically the corresponding driven equation by using a generalized Sturmian approach in which the asymptotic conditions of the wave functions are imposed by defining the basis appropriately. Both spherical [15–17] and hyperspherical [18,19] formulations—which are fully independent—will be used and compared favorably. For the Orsay high-incident-energy conditions [1,2], we shall present cross sections which could serve as benchmark values.

Model calculations, used as benchmarks, can be found throughout the collision literature. They are useful, in general, as they allow one to put on a strong footing different numerical methods which do not necessarily yield converging results when applied to complicated scattering processes which involve several ingredients. For the three-body problem, before solving the full e^--H ionization problem, the *S*-wave model (often referred to as the Temkin-Poet model [20,21]) calculations have played a very important role in the development of theoretical methods. Very recently, a Coulombic three-body breakup model was presented [22,23] allowing for detailed investigations of convergence issues. In a similar way, it is to be expected that a four-body e^--He *S*-wave model will play an equally important role for understanding double ionization, as well as ionization with excitation. Although restricted to zero angular momentum states, an *S*-wave model serves as a test bed. It contains most of the features and difficulties associated to the full problem of treating electron collisions with a target that has two active electrons, but requires less computational resources. One such model was investigated in Ref. [24], where the authors focused on double ionization at around 200 eV incident energy. In Ref. [25], Plottke and co-workers made a systematic study of single ionization from threshold to several hundred electron volts; all electrons were not treated in an equivalent manner. A similar model was considered by Horner and co-workers [26], who studied excitation and single ionization with low projectile energies. Recently, the propagating exterior complex scaling method was used to explore several four-body processes within the Temkin-Poet model [27,28]. The authors made a very complete study of excitation, excitation ionization, and also double ionization. Their nonperturbative solution was calculated with high accuracy, and their results should certainly be considered as solid benchmark values. However, in the case of double ionization—the process we are interested in—the presented cross sections do not correspond to the case where the two ejected electrons share a given amount of energy. Besides, the maximum projectile energy considered was 500 eV, a value quite distant from the one considered in the Orsay experiments. All the mentioned model calculations are very important for the low-incident-energy range where both experimental data and theoretical calculations are available. In particular, the four-body results of Bartlett and Stelbovics [27,28] will surely play a determinant role as those of the Temkin-Poet model played for the three-body case. Finally, for completeness, we should also mention that, even more recently, *J*-matrix calculations of electron-helium *S*-wave scattering (single excitation and ionization) have been presented by Konovalov *et al.* [29].

In the present contribution, we focus on the double-ionization process due to high-energy electron impact (Orsay experimental conditions), exploring therefore a very different—and thus complementary—domain. None of the above cited references performed calculations in this energy range; even within a Temkin-Poet approach, any of the methods would require huge computational resources. Besides, it should be noted that in the Orsay kinematical situations, the ejected electrons are sharing a rather small amount of energy given to the target, since the projectile is scattered with a fixed high energy. In this case, the four-body problem turns into

a three-body one, and it is for this reduced problem that the S-wave model is discussed here. Our study aims to test the three-body problem and not the four-body one as done, for example, by Bartlett and Stelbovics [27,28]. As previously stated, it is within the three-body problem that disagreement is found when describing the $(e,3e)$ processes measured by the Orsay group.

Another point of interest, which has suscitated considerable discussion in the $(e,3e)$ community (see, e.g., [30]), is to investigate the energy region where the full four-body problem starts to be in agreement with the high-energy (three-body problem) approach. For this purpose, we shall also provide benchmark data at 500 eV incident energy, the maximum value considered in Refs. [27,28]. At this energy we do not expect the first Born approximation to be valid, and a four-body nonperturbative calculation should be able to clearly illustrate this.

The rest of the paper is organized as follows. In Sec. II we present the theoretical background for the treatment of the double ionization of helium by high-energy electron impact. We also provide the necessary formulas to extract the transition amplitude from the asymptotic behavior of the wave function. In Sec. III a simplified version, the S-wave model, of the $(e,3e)$ process is introduced and solved using generalized Sturmian basis functions. Two independent formulations provide equal benchmark cross sections for the experimental configurations of Refs. [1,2], and for the 500 eV case. Concluding remarks are given in Sec. IV.

Atomic units ($\hbar = e = 1$) are assumed throughout, unless stated otherwise.

II. GENERAL THEORY

The nonrelativistic four-body Hamiltonian for three electrons and an infinite mass helium nucleus of charge $Z = 2$ is given by

$$H = -\frac{1}{2}\nabla_1^2 - \frac{1}{2}\nabla_2^2 - \frac{1}{2}\nabla_3^2 - \frac{Z}{r_1} - \frac{Z}{r_2} - \frac{Z}{r_3} + \frac{1}{r_{12}} + \frac{1}{r_{13}} + \frac{1}{r_{23}}, \tag{3}$$

where particle 1 labels the electron projectile, while particles 2 and 3 are the target electrons. In view of the presentation below, we also define the Hamiltonians:

$$h_{\rm He} = \left(-\frac{1}{2}\nabla_2^2 - \frac{1}{2}\nabla_3^2 - \frac{Z}{r_2} - \frac{Z}{r_3} + \frac{1}{r_{23}}\right), \tag{4a}$$

$$h_p(Z_p) = \left(-\frac{1}{2}\nabla_1^2 - \frac{Z_p}{r_1}\right). \tag{4b}$$

$h_{\rm He}$ is the three-body helium Hamiltonian [subsystem (2,3)], while $h_p(Z_p)$ is the Hamiltonian associated to the projectile including only Coulomb projectile-nucleus interaction with a model charge Z_p. With these definitions, we decompose the four-body Hamiltonian as follows:

$$H = H_0(Z_p) + \bar{W}(Z_p), \tag{5}$$

where

$$H_0(Z_p) = h_p(Z_p) + h_{\rm He}, \tag{6a}$$

$$\bar{W}(Z_p) = -\frac{Z - Z_p}{r_1} + \frac{1}{r_{12}} + \frac{1}{r_{13}}. \tag{6b}$$

On top of all kinetic operators, the Hamiltonian $H_0(Z_p)$ includes all the interactions of the subsystem (2,3) through $h_{\rm He}$, and a projectile-nucleus interaction $-Z_p/r_1$ through $h_p(Z_p)$. The two subsystems are coupled through the interaction $\bar{W}(Z_p)$.

To study $(e,3e)$ collision processes we need to find a scattering solution, with outgoing $(+)$ type behavior, of the four-body Schrödinger equation

$$[H_0 + \lambda\bar{W} - E]\Psi(\mathbf{r}_1,\mathbf{r}_2,\mathbf{r}_3) = 0, \tag{7}$$

where explicit dependence on Z_p has been dropped off. The inclusion of the parameter λ (whose numerical value is 1) associated to the interaction $\bar{W}$ suggests the following expansion:

$$\Psi^+ = \sum_n \lambda^n \Psi^{(n)+}, \tag{8}$$

where successive orders $\Psi^{(n)+}$ satisfy the following system of differential equations:

$$[E - H_0]\,\Psi^{(0)+}(\mathbf{r}_1,\mathbf{r}_2,\mathbf{r}_3) = 0, \tag{9a}$$

$$[E - H_0]\,\Psi^{(1)+}(\mathbf{r}_1,\mathbf{r}_2,\mathbf{r}_3) = \bar{W}\Psi^{(0)+}(\mathbf{r}_1,\mathbf{r}_2,\mathbf{r}_3), \tag{9b}$$

$$\vdots$$

$$[E - H_0]\,\Psi^{(n)+}(\mathbf{r}_1,\mathbf{r}_2,\mathbf{r}_3) = \bar{W}\Psi^{(n-1)+}(\mathbf{r}_1,\mathbf{r}_2,\mathbf{r}_3). \tag{9c}$$

From the zeroth-order equation (9a), $\Psi^{(0)+}(\mathbf{r}_1,\mathbf{r}_2,\mathbf{r}_3)$ is the solution of the Hamiltonian H_0 which is separable in the two subsystems (2,3) and 1 [see Eq. (6a)]. Let $\Phi^{(0)}(\mathbf{r}_2,\mathbf{r}_3)$ represent the ground state of the helium atom, and consider an incident projectile of momentum $\mathbf{k}_i$. The solution $\Psi^{(0)+}(\mathbf{r}_1,\mathbf{r}_2,\mathbf{r}_3)$, which represents the initial state of the system, reads

$$\Psi^{(0)+}(\mathbf{r}_1,\mathbf{r}_2,\mathbf{r}_3) = \begin{cases} \frac{1}{(2\pi)^{3/2}} e^{i\mathbf{k}_i\cdot\mathbf{r}_1}\Phi^{(0)}(\mathbf{r}_2,\mathbf{r}_3), & Z_p = 0, \\ C(Z_p,\mathbf{k}_i,\mathbf{r}_1)\Phi^{(0)}(\mathbf{r}_2,\mathbf{r}_3), & Z_p = Z. \end{cases} \tag{10}$$

The projectile-nucleus interaction is either switched off ($Z_p = 0$), and a plane wave describes the incident projectile, or properly represented through a Coulomb wave function $C(Z_p,\mathbf{k}_i,\mathbf{r}_1)$ with charge $Z_p = Z$ [31].

Next, consider the first-order solution of Eq. (9b) in which the driven term is clearly not separable as $\bar{W}$ couples all the coordinates. A formal solution is

$$\Psi^{(1)+} = G_0\bar{W}\Psi^{(0)+}, \tag{11}$$

where $G_0 = [E - H_0]^{-1}$ is the Green's function corresponding to the Hamiltonian H_0. The interaction $\bar{W}$ is included only once in (9b), or (11), meaning that the projectile and the target electrons interact only once. Using again the definition of the Hamiltonian H_0, we can look for solutions written as

$$\Psi^{(1)+}(\mathbf{r}_1,\mathbf{r}_2,\mathbf{r}_3) = \int d\mathbf{k}\, C(Z_p,\mathbf{k},\mathbf{r}_1)\Phi^{(1)+}_{sc}(\mathbf{r}_2,\mathbf{r}_3), \tag{12}$$

where the label sc stands for scattering. Let E_a be the energy of two electrons in interaction with the nucleus in the final

state, and $k^2/2$ the energy associated to the projectile: the total energy of the system is then $E = k^2/2 + E_a$. Replacing the proposal (12) in Eq. (9b), and taking into account that $h_p(Z_p)C(Z_p,\mathbf{k},\mathbf{r}_1) = (k^2/2)C(Z_p,\mathbf{k},\mathbf{r}_1)$, we have

$$\int d\mathbf{k}\, C(Z_p,\mathbf{k},\mathbf{r}_1)\,[E_a - h_{He}]\,\Phi_{sc}^{(1)+}(\mathbf{r}_2,\mathbf{r}_3) = \bar{W} C(Z_p,\mathbf{k}_i,\mathbf{r}_1)\Phi^{(0)}(\mathbf{r}_2,\mathbf{r}_3)\,, \tag{13}$$

where the integration limits are restricted by energy conservation. Projecting by the left with a Coulomb function $C(Z_p,\mathbf{k}_f,\mathbf{r}_1)$ with momentum $\mathbf{k}_f$, i.e., selecting $\mathbf{k}_f$ as being the momentum of the scattered projectile in the final channel, we find

$$[E_a - h_{\rm He}]\,\Phi_{sc}^{(1)+}(\mathbf{r}_2,\mathbf{r}_3) = W_{fi}(\mathbf{r}_2,\mathbf{r}_3)\,\Phi^{(0)}(\mathbf{r}_2,\mathbf{r}_3)\,, \tag{14}$$

where in the right-hand side (RHS)

$$W_{fi}(\mathbf{r}_2,\mathbf{r}_3) = \langle \mathbf{k}_f|\bar{W}|\mathbf{k}_i\rangle = \begin{cases} \frac{1}{(2\pi)^3}\frac{4\pi}{q^2}(-Z + e^{i\mathbf{q}\cdot\mathbf{r}_2} + e^{i\mathbf{q}\cdot\mathbf{r}_3}), & Z_p = 0, \\ \langle C(Z_p,\mathbf{k}_f,\mathbf{r}_1)|\frac{1}{r_{12}} + \frac{1}{r_{13}}|C(Z_p,\mathbf{k}_i,\mathbf{r}_1)\rangle, & Z_p = Z. \end{cases} \tag{15}$$

In this way we have reduced the four-body problem to a pure three-body one where the dynamics of the two ejected electrons in the presence of the heavy nucleus is described by Eq. (14). This is a pure three-body problem. As we pointed out in the Introduction it has been said that the three-body scattering problem has been completely solved numerically with various numerical methods. However, when the same recipes are applied to a problem similar to Eq. (14), the same agreement is not observed, and we wonder what are the difficulties leading to such discrepancies. It is easy to show that the problem (14) is well formulated and that its solution possesses all the information contained in the first Born approximation. The formal solution of Eq. (14) may be written as

$$\Phi_{sc}^{(1)+}(\mathbf{r}_2,\mathbf{r}_3) = \int d\mathbf{r}_2' d\mathbf{r}_3' G_a^+(\mathbf{r}_2,\mathbf{r}_3,\mathbf{r}_2',\mathbf{r}_3') W_{fi}(\mathbf{r}_2',\mathbf{r}_3')\Phi^{(0)}(\mathbf{r}_2',\mathbf{r}_3'), \tag{16}$$

where $G_a^+(\mathbf{r}_2,\mathbf{r}_3,\mathbf{r}_2',\mathbf{r}_3')$ is the three-body Coulomb Green's function. In the Ω_0 region its asymptotic limit reads [32]

$$G_a^+(\mathbf{r}_2,\mathbf{r}_3,\mathbf{r}_2',\mathbf{r}_3') \to \frac{(2\pi i)^{1/2}}{(2\pi)^3}\kappa^{\frac{3}{2}}\frac{e^{i[\kappa\rho - \lambda_0\ln(2\kappa\rho) - \sigma_0]}}{\rho^{\frac{5}{2}}}\Psi^-_{\tilde{\mathbf{k}}_2,\tilde{\mathbf{k}}_3}(\mathbf{r}_2',\mathbf{r}_3'), \tag{17}$$

where $\rho = (r_2^2 + r_3^2)^{1/2}$ is the hyper-radius, $\kappa = (2E)^{1/2}$, σ_0 is a phase, and λ_0 is a Coulomb parameter [32]; $\tilde{\mathbf{k}}_j$ $(j = 2,3)$ are the coordinate-dependent momenta defined originally by Alt and Mukhamedzhanov [33]. Hence

$$\Phi_{sc}^{(1)+}(\mathbf{r}_2,\mathbf{r}_3) \to \frac{(2\pi i)^{1/2}}{(2\pi)^3}\kappa^{\frac{3}{2}} T_{\tilde{\mathbf{k}}_2,\tilde{\mathbf{k}}_3}\frac{e^{i[\kappa\rho - \lambda_0\ln(2\kappa\rho) - \sigma_0]}}{\rho^{\frac{5}{2}}}, \tag{18}$$

where the transition amplitude $T_{\tilde{\mathbf{k}}_2,\tilde{\mathbf{k}}_3}$ is given by

$$T_{\tilde{\mathbf{k}}_2,\tilde{\mathbf{k}}_3} = \begin{cases} \frac{1}{(2\pi)^3}\frac{4\pi}{q^2}\langle\Psi^-_{\tilde{\mathbf{k}}_2,\tilde{\mathbf{k}}_3}(\mathbf{r}_2,\mathbf{r}_3)\,|\,-Z + e^{i\mathbf{q}\cdot\mathbf{r}_2} + e^{i\mathbf{q}\cdot\mathbf{r}_3}|\Phi^{(0)}(\mathbf{r}_2,\mathbf{r}_3)\rangle, & Z_p = 0, \\ \langle\Psi^-_{\tilde{\mathbf{k}}_2,\tilde{\mathbf{k}}_3}(\mathbf{r}_2,\mathbf{r}_3)\,|\langle C(Z_p,\mathbf{k}_f,\mathbf{r}_1)|\frac{1}{r_{12}} + \frac{1}{r_{13}}|C(Z_p,\mathbf{k}_i,\mathbf{r}_1)\rangle|\Phi^{(0)}(\mathbf{r}_2,\mathbf{r}_3)\rangle, & Z_p = Z. \end{cases} \tag{19}$$

These transition amplitudes are equivalent to the one given by Eq. (2), except for the presence of the position-dependent momenta $\tilde{\mathbf{k}}_2$ and $\tilde{\mathbf{k}}_3$. For $Z_p = 0$, one recovers the standard first Born approximation, as used in all the calculations presented in the literature. The case $Z_p = Z$, on the other hand, includes the projectile-nucleus interaction in both initial and final channels. In ion-atom collision processes a similar approach has been implemented [34].

III. A SIMPLE MODEL

A. Formulation of the problem

Instead of considering the solution for the full first-order equation (14), we consider here the following S-wave model:

$$\left[-\frac{1}{2r_2^2}\frac{\partial}{\partial r_2}\left(r_2^2\frac{\partial}{\partial r_2}\right) - \frac{1}{2r_3^2}\frac{\partial}{\partial r_3}\left(r_3^2\frac{\partial}{\partial r_3}\right) - \frac{Z}{r_2} - \frac{Z}{r_3} + \frac{1}{r_>} - E_a\right]\phi_{sc}^{(1)+}(r_2,r_3) = \mathcal{F}(r_2,r_3)\,. \tag{20}$$

Furthermore, for simplicity, we consider only the case $Z_p = 0$. This leads to the following definition for the RHS:

$$\mathcal{F}(r_2,r_3) = -\frac{1}{(2\pi)^3}\frac{4\pi}{q^2}[-Z + j_0(qr_2) + j_0(qr_3)]\phi^{(0)}(r_2,r_3), \tag{21}$$

where $j_0(x)$ represents the spherical Bessel function of zeroth order. In (21), $\phi^{(0)}(r_2,r_3)$ is the ground-state solution of the S-wave helium equation (20) with the RHS set to zero.

B. Spherical Sturmian expansion

To solve Eq. (20) we use a configuration interaction (CI) expansion

$$\phi_{sc}^{(1)+}(r_2,r_3) = \sum_\nu a_\nu^s\theta_\nu^+(r_2,r_3)\,, \tag{22}$$

where a_ν^s are linear coefficients with index $\nu = \{n_2,n_3\}$; the configurations are expressed in terms of products of generalized Sturmian functions $S_{n_i}^+(r_i)$ with outgoing-wave

boundary conditions [15,16],

$$\theta_\nu^+(r_2,r_3) = \frac{1}{r_2 r_3}\frac{1}{\sqrt{2}}\left[S_{n_2}^+(r_2)S_{n_3}^+(r_3) + (-1)^S S_{n_2}^+(r_3)S_{n_3}^+(r_2)\right], \tag{23}$$

where S is the total spin. The basis functions $S_{n_i}^+(r_i)$ $(i = 2,3)$ are solutions of a two-body radial equation,

$$\left[-\frac{1}{2}\frac{d^2}{dr_i^2} + U_i(r_i) - E_i\right] S_{n_i}^+(r_i) = -\beta_{n_i} V(r_i) S_{n_i}^+(r_i), \tag{24}$$

where $V(r_i)$ is a short-range generating potential, i.e., $V(r_i) \to 0$ for $r_i > r_c$. On the other hand, we include a potential $U_i(r_i)$ which has a Coulomb tail $-Z_i/r_i$ for $r_i > r_c$. This implies that the asymptotic behavior of the basis functions is associated to an outgoing wave of energy E_i, distorted by the charge Z_i. Equation (24) generates a *discrete spectrum* with complex eigenvalues β_i, and a complete set of basis functions which are orthogonal with respect to $V(r_i)$ [17].

An expansion such as (22) has been used successfully in a recent study of e^--H single ionization [16]; it was shown that the best way of defining the asymptotic behavior in each coordinate r_i corresponds to $E_i = E$ and $Z_i = Z - 1$. We observed that this choice is also adequate for the present $(e,3e)$ processes. It actually corresponds to an appropriate description for the Ω_α region: one particle is at finite distances with close-to-zero energy and sees the full nuclear charge Z, while the other is at infinite distances carrying all the system energy but sees a screened charge Z_i. Since this screened value does not correspond to the atomic value at short distances, in order to have a more consistent picture, we define the potential $U_i(r_i)$ by parts, i.e., $U_i(r_i) = -Z/r_i$ for the inner region $(r < r_c)$, and $U_i(r_i) = -(Z-1)/r_i$ for the outer region $(r > r_c)$ (no major differences were observed between the results obtained with smooth or sharp charge transitions). The choice of the outer charge has a considerable effect in yielding a CI expansion convergence towards the correct asymptotic behavior and, at the same time, a smooth inner solution. On the other hand, the inner charge is not so important since in the inner region the expansion has to deal with the potentials not removed by the basis elements; by choosing $Z_i = Z$ in the inner region, though, the Sturmian functions diagonalize not only the the kinetic energy but also the electron-nucleus potentials Z/r_i.

We underline here that the chosen charges are used only for the basis elements construction. In the three-body Schrödinger equation the Coulomb potential with $Z = 2$ has to be solved.

C. Hyperspherical Sturmian expansion

We also perform a different numerical expansion in generalized hyperspherical Sturmian (GHS) functions. Since the GHS method has received ample documentation in our previous work (see, for example, [18,19,22,23]), we will confine ourselves to outline only its most important features. More detailed work related to the present particular S-wave $(e,3e)$ problem and the analysis of convergence properties is the subject of current investigations and will be presented in a forthcoming article. The hyperspherical coordinates consist on a hyper-radius ρ and five hyperangular coordinates. Leaving aside the polar angles, we shall simply use $\rho = \sqrt{r_2^2 + r_3^2}$ and the hyperangle $\alpha = \arctan(r_3/r_2)$. Within this framework, the form of the expansion, analog to the spherical expansion (22), is

$$\phi_{sc}^{(1)+}(\rho,\alpha) = \sum_\nu a_\nu^{hs}\hat{\theta}_\nu^+(\rho,\alpha), \tag{25}$$

where a_ν^{hs} are linear coefficients with index $\nu = \{n,m\}$; the configurations are expressed in terms of products of hyperradial (quantum numbers m) and hyperangular (quantum numbers n) functions:

$$\hat{\theta}_\nu^+(\rho,\alpha) = \frac{1}{\rho^{5/2}}\hat{S}_{n,m}^+(\rho)\Omega_n(\alpha). \tag{26}$$

The hyperangular functions are the solutions of the hyperangular eigenvalue equation,

$$\Lambda^2\Omega_n(\alpha) = \lambda_n(\lambda_n + 4)\Omega_n(\alpha), \tag{27}$$

where Λ^2 is the S-wave simplified form of the grand angular operator, and $\lambda_n = 2n$ (for integer numbers $n = 0,1,\ldots$). These functions have an analytical expression in terms of Jacobi polynomials [18],

$$\Omega_n(\alpha) = \mathcal{N}_n\, {}_2F_1\left(-n,n+2,\frac{3}{2};\sin^2\alpha\right), \tag{28}$$

with $\mathcal{N}_n = 4(n+1)/\sqrt{\pi}$. The eigenfunctions $\Omega_n(\alpha)$ form a complete set and satisfy the orthonormality relation

$$\int_0^{\pi/2}\Omega_n(\alpha)\Omega_m(\alpha)\sin^2\alpha\,\cos^2\alpha\,d\alpha = \delta_{nm}. \tag{29}$$

Coupled to these angular polynomials, for a given n, we take as hyper-radial basis functions the Sturmian functions $\hat{S}_{n,m}^+(\rho)$ satisfying an equation analog to Eq. (24),

$$\left[-\frac{1}{2}\frac{d^2}{d\rho^2} + \frac{\lambda_n(\lambda_n+4)+\frac{15}{4}}{2\rho^2} + U_\rho(\rho) - E\right]\hat{S}_{n,m}^+(\rho) = -\hat{\beta}_{n,m}\,V_\rho(\rho)\,\hat{S}_{n,m}^+(\rho), \tag{30}$$

together with the boundary conditions:

$$\hat{S}_{n,m}^+(0) = 0 \qquad \lim_{\rho\to\infty}\hat{S}_{n,m}^+(\rho) \propto e^{i(K\rho - \frac{Z}{K}\ln 2K\rho)}, \tag{31}$$

where E is a parameter which will be set equal to the system's energy, $K = \sqrt{2E}$ is the hyperspherical generalized momentum, and $\hat{\beta}_{n,m}$ are the eigenvalues. The generating potential $V_\rho(\rho)$ is of short range, and vanishes faster than ρ^{-1} as $\rho \to \infty$. In that way, we can choose the auxiliary potential $U_\rho(\rho)$ as a Coulomb potential with charge Z, imposing the desired asymptotic outgoing Peterkop's boundary condition to the basis functions [note the similarities in the asymptotic condition defined in Eq. (31) and that given in Eq. (18)]. Without loss of generality, we can generate hyperadial Sturmian functions with no angular momentum λ_n in Eq. (30).

D. Linear system

Replacing the CI expansions (22) or (25) in the scattering equation (20), and projecting onto the basis elements, we obtain linear systems of the form

$$[\mathbf{H} - (E - \tilde{E})\mathbf{O}]\mathbf{a}^+ = \mathcal{F}, \tag{32}$$

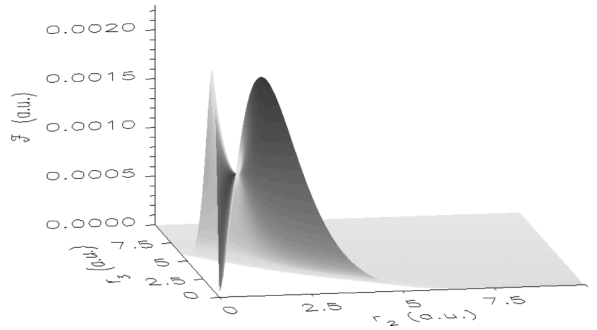

FIG. 1. Driven term $\mathcal{F}(r_2,r_3)$ defined by Eq. (21) for $q = 0.24$ a.u.

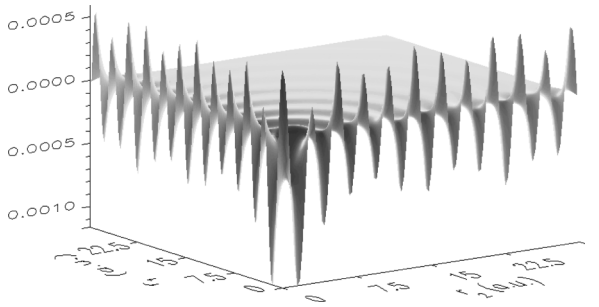

FIG. 2. Real part of the scattering wave function $\Phi_{sc}^{(1)+}(r_2,r_3)\sqrt{r_2^2+r_3^2}$ as a function of the ejected electrons radial coordinates r_2 and r_3. $\Phi_{sc}^{(1)+}$ is the solution of Eq. (20) for an energy $E_a = 0.791$ a.u. and for a momentum transfer $q = 0.24$ a.u.

where **H** and **O** are the matrix representation of the Hamiltonian and overlap ($[\mathbf{H}]_{\nu\nu'} = \langle\theta_\nu|H|\theta_{\nu'}\rangle$, $[\mathbf{O}]_{\nu\nu'} = \langle\theta_\nu|\theta_{\nu'}\rangle$), and $\mathcal{F}$ represents the RHS projected onto the basis set; $\mathbf{a}^+$ is the vector of coefficients that build the solution. For the spherical expansion $\tilde{E} = E_2 + E_3$; as the best choice of the Sturmian parameters is $E_2 = E_3 = E$, the overlap matrix elements have to be calculated. In the hyperspherical expansion, $\tilde{E} = E$, so overlap matrix elements need not be computed in this case.

Both basis sets are constructed in such a way that they remove the kinetic energy term of Eq. (20). In the region $r_i < r_c$, the spherical Sturmian functions diagonalize also the interaction potentials Z/r_i; in the outer region $r_i > r_c$, both the overlap and Coulomb tail potential matrix elements (see above discussion on the choice of Z_i) can be evaluated analytically (see [16,35]). Therefore, only the interaction $1/r_>$, the auxiliary potentials $V_i(r)$, and the overlaps (finite range integrals) remain to be computed, substantially simplifying the evaluation of the matrix elements $[\mathbf{H}]_{\nu\nu'}$. In the hyperspherical approach, the latter involve separable integrals.

The driven term $\mathcal{F}(r_2,r_3)$ defined by Eq. (21) includes the ground state $\phi^{(0)}(r_2,r_3)$ of the S-wave helium (exact energy $E_0 \simeq -2.879$ a.u.). This ground state can be calculated very accurately, as we did for example in Refs. [36,37]. The degree of sophistication (correlation) in its description will obviously affect the final cross sections corresponding to the proposed S-wave $(e,3e)$ model. However, the main focus here is on the double continuum wave function and besides we want to produce cross-section data that can be easily reproduced by other numerical methods; it is thus better to avoid any unnecessary source of divergences between different calculations. For this reason, we take as ground state the simple product of screened exponentials: $\phi^{(0)}(r_2,r_3) = (Z_e^3/\pi)e^{-Z_e(r_2+r_3)}$ with $Z_e = Z - 5/16$, which yields a ground-state energy of $E_0 \simeq -2.847$ a.u.

Due to the bound character, when the coordinates r_2 and r_3 are larger than $R_0 \simeq 5$ a.u. the full term $\mathcal{F}(r_2,r_3)$ is practically zero. This is illustrated in Fig. 1 where $\mathcal{F}(r_2,r_3)$ is plotted as a function of r_2 and r_3, with $q = 0.24$ a.u.; this momentum transfer corresponds to the initial and final projectile energies of, respectively, $E_i = 5599$ eV and $E_f = 5500$ eV, and a deflection of 0.45°, used in the Orsay experiment [1]. These values, together with the exact ground-state energy of the bound initial state, define the energy of the final three-body subsystem (2,3) equal to 0.734 a.u. ($\simeq 20$ eV). For an equal energy sharing situation, this corresponds to 10 eV per electron, as in the experiments [1]. We also considered the other experimental situation [2] corresponding to a momentum transfer equal to $q = 0.22$ a.u., together with a two-electron system with energy 0.294 a.u. ($\simeq 8$ eV) (4 eV per electron in equal energy sharing).

E. Scattering wave function

We have calculated the (singlet, $S = 0$) solution $\Phi_{sc}^{(1)+}$ of Eq. (20) with the two Sturmian expansions: in spherical coordinates [Eq. (23)] and hyperspherical coordinates [Eq. (26)]. It must be emphasized that the two methods have been implemented in completely independent numerical codes.

In order to visualize the scattering solution, we show in Fig. 2 the real part of $\Phi_{sc}^{(1)+}$ times $\sqrt{r_2^2+r_3^2}$. This factor was chosen in order to maintain a uniform outgoing amplitude. For all the results shown in the present section, we use the approximate energy of the He ground state. Therefore, for the momentum transfer $q = 0.24$ a.u., we solve Eq. (20) for an energy value $E_a = 0.791$ a.u.. Details of the real part of the solution can be seen in the contour plots presented in Fig. 3. The function $\Phi_{sc}^{(1)+}\rho^{5/2}$ is plotted as a function of r_2 and r_3. Here the factor $\rho^{5/2}$ was chosen in order to keep the amplitude of the ionization (the hyperspherical outgoing wave) uniform as $\rho \to \infty$; it has to be noted that this factor increases the amplitude of single-ionization channels (the peaks close the axis $r_2 = 0$ or $r_3 = 0$, i.e., the Ω_α regions) by the factor $\rho^{1/2}$. The result of the spherical expansion is shown in the left panel. In the domain $r_2,r_3 > R_0$, in which the driven term vanishes, the equation admits the solution of the corresponding homogeneous equation. The basis functions $\theta_\nu^+(r_2,r_3)$ for r_i values larger than r_c are simply products of outgoing waves in spherical coordinates. However, as can be observed in the figure, in the inner region they manage to generate the appropriate solution with a hyperspherical outgoing front (a formal and mathematical explanation of how the hyperspherical front is constructed from a spherical treatment is under investigation by our group). For comparison, the result obtained with the second numerical approach—the hyperspherical expansion—is shown in the right panel. Considering that the solution is obtained with two completely independent programs, the agreement between both calculations is remarkable.

This agreement can be further appreciated through a more detailed and quantitative comparison between both numerical methods. Figure 4 shows slices of the solution $\Phi_{sc}^{(1)+}\rho^{5/2}$ as

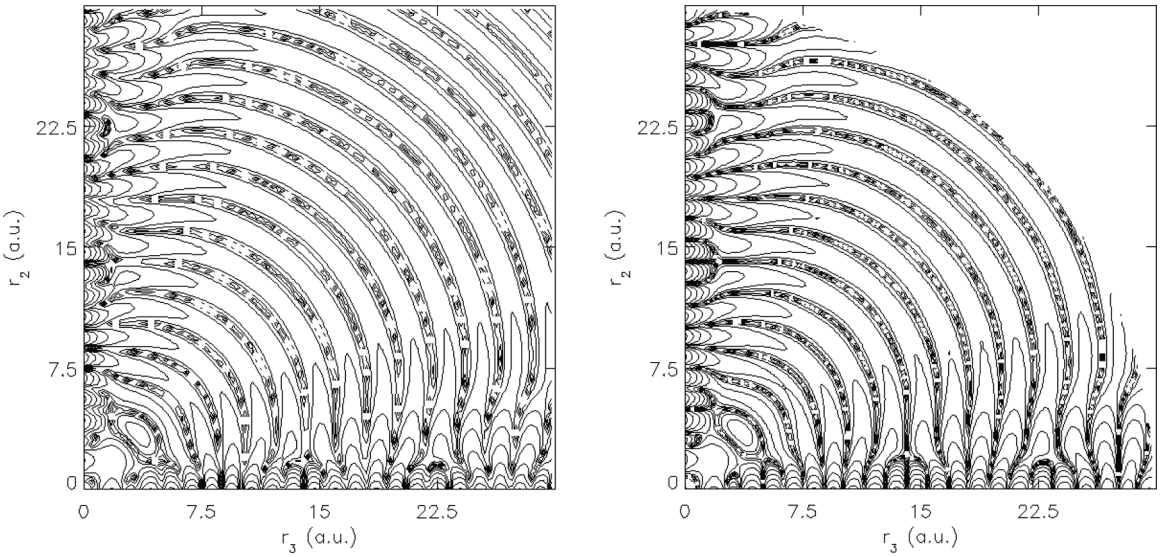

FIG. 3. Left: real part of the scattering wave function $\Phi_{sc}^{(1)+}(r_2,r_3)\rho^{5/2}$ as a function of the ejected electrons radial coordinates r_2 and r_3, for $E_a = 0.791$ a.u. and $q = 0.24$ a.u. Right: real part of $\Phi_{sc}^{(1)+}(\rho,\alpha)\rho^{5/2}$.

a function of the hyper-radius ρ, for different values of of the hyperangle α. The comparisons are made at low angles (i.e., close to the r_2 and r_3 axis), where the differences between spherical and hyperspherical functions are the largest in magnitude. The worst case scenario produces a difference of less than a 5%. We also show the comparison between both calculations for $r_2 = r_3$ (i.e., at $\alpha = \pi/4$), a region in which—although the amplitudes of the solutions are very low—the agreement between the results given by the two numerical approaches is excellent.

Since we aim to provide reproducible data, we have chosen to solve the driven equation (20) with a very simple ground state of the S-wave helium on the RHS. We have, however, also performed a calculation using the most accurate wave function we are able to calculate [37]. The ensuing scattering wave function does not change significatively except for the global amplitude and some changes, mostly observed in the (Ω_α) regions close to the axis.

F. Differential cross section

One of our goals is to provide e^--He double-ionization benchmark data within the above S-wave model. As shown in Sec. II, the transition amplitude for the double-ionization process can be extracted from the asymptotic limit of the wave function $\phi_{sc}^{(1)+}(r_2,r_3)$. This applies also for the simplified model under consideration. Evaluating $\bar{\phi}_{sc}^{(1)+}(\rho,\alpha) = \phi_{sc}^{(1)+}(\rho,\alpha)\,\rho^{5/2}$ at large values of ρ and taking its square modulus gives the transition amplitude

$$|T_{fi}|^2 = \frac{(2\pi)^5}{\kappa^3}\left|\bar{\phi}_{sc}^{(1)+}(\rho\to\infty,\alpha)\right|^2. \tag{33}$$

This is equivalent to taking the S-wave component of the wave function $\Psi^-_{\vec{\mathbf{k}}_2,\vec{\mathbf{k}}_3}(\mathbf{r}'_2,\mathbf{r}'_3)$ of (17), and thus the S-wave component of the transition amplitude defined by the integral (19). The extraction of the amplitude directly from the wave function (similarly to other flux formulas [38]) provides the advantage that it allows one to verify the accuracy of the solution.

With the transition amplitude (33) and the definition of the $(e,3e)$ cross section (1), we obtain

$$\sigma(q,\alpha) = \lim_{\rho\to\infty}\sigma_\rho(q,\alpha) = \lim_{\rho\to\infty}\frac{(2\pi)^9}{\kappa}\frac{k_f}{k_i}\left|\bar{\phi}_{sc}^{(1)+}(\rho,\alpha)\right|^2\cos\alpha\,\sin\alpha, \tag{34}$$

where $k_2 = \kappa\,\cos\alpha$ and $k_3 = \kappa\,\sin\alpha$; α defines how the energy is shared between the two ejected electrons. For a given q value, $\sigma(q,\alpha)$ is a singly differential cross section. It should be independent of the hyper-radial coordinate; effectively, one evaluates numerically σ_ρ at different values of ρ and then extrapolates the result to infinite distances with a form $\sigma \simeq \sigma_\rho + O[\rho^{-1}]$ [39]. This technique was used successfully for the S-wave Temkin-Poet model for the electron-hydrogen ionization [15,16,40]. For each fixed value of ρ we have a circular arc contour in the (r_2,r_3) plane through which the local energy fraction $\epsilon = \sin^2\alpha = E_3/E$ changes from 0 to 1 ($\alpha = 0$ to $\pi/2$). Note that on the borders (ϵ close to 0 and 1) this contour hits discrete single-ionization channels which are coupled with that of the double ionization, and evaluation of the singly differential cross section (SDCS) with this definition of the energy fraction leads to unphysical behavior at the unequal energy sharing regime [40].

Instead of this standard definition, we used an energy fraction value derived from the components of the quantum-mechanical flux operator:

$$\epsilon = \frac{J_2^2}{J_2^2 + J_3^2}, \tag{35}$$

where

$$J_i = \frac{1}{2i}\left[(\Psi_{sc}^+)^*\frac{\partial\Psi_{sc}^+}{\partial r_i} - \Psi_{sc}^+\frac{\partial(\Psi_{sc}^+)^*}{\partial r_i}\right], \quad i = 2,3. \tag{36}$$

This alternative definition (whose foundation is described in a separate contribution [41]) avoids the unphysical cross-section behavior [42] at ϵ values close to 0 and 1.

For fixed values of q, we have calculated SDCS for double ionization of the S-wave helium model. We evaluated, on a

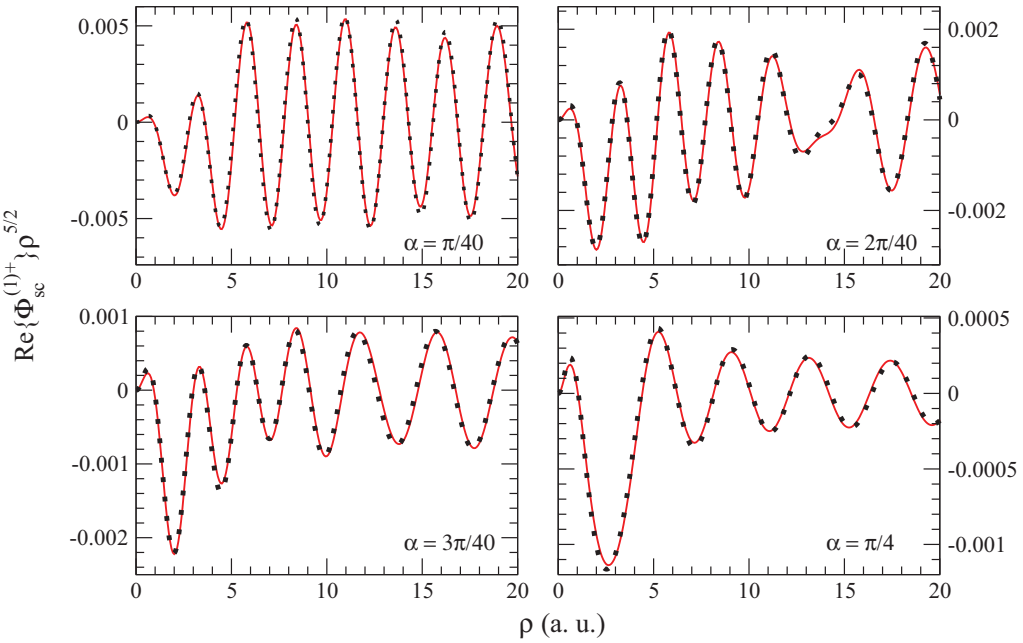

FIG. 4. (Color online) Real part of the scattering wave function $\Phi_{sc}^{(1)+}\rho^{5/2}$ as a function of the ejected electrons hyperspherical coordinate ρ for different values of the hyperangle α, obtained with the spherical (red, continuous) and hyperspherical (black, dotted) coordinates Sturmian expansions. $E_a = 0.791$ a.u. and $q = 0.24$ a.u.

uniform α grid, both the energy fraction (35) and the cross section (34). In Figs. 5 and 6, we present for $q = 0.24$ a.u. and $q = 0.22$ a.u., respectively, SDCS results obtained for different increasing values of ρ, from 2λ to 12λ, increasing by steps of $\lambda = 2\pi/\sqrt{2E}$, associated with the two-electron system wavelength. We can see that the curves slowly converge towards the extrapolated ($\rho \to \infty$) curve (circles); we have verified that by increasing the number of steps no significant differences were observed when using the $\rho \to \infty$ extrapolation technique. Four more observations stem from the figure: the smoothness of the scattering solution is reflected into smooth SDCS curves; no unphysical behavior is observed near $\epsilon = 0$ or $\epsilon = 1$; these SDCS are continuous at $\epsilon = 0.5$ as it should be; the cross sections have a rather small magnitude which can be associated to the high energy of the incoming electron. When using a highly correlated S-wave helium ground state instead of the simple product of exponentials, the cross-section magnitudes change only slightly. No comparison with other calculations can be presented since these are the first calculations of the process at the considered projectile energy. As the calculated SDCS are to be considered as benchmark values, they are provided in tabular form (Table I) for the two values of q considered.

As mentioned in the Introduction, it is useful to consider also lower impact energies in order to make a connection with the precise nonperturbative approach [27,28]. However,

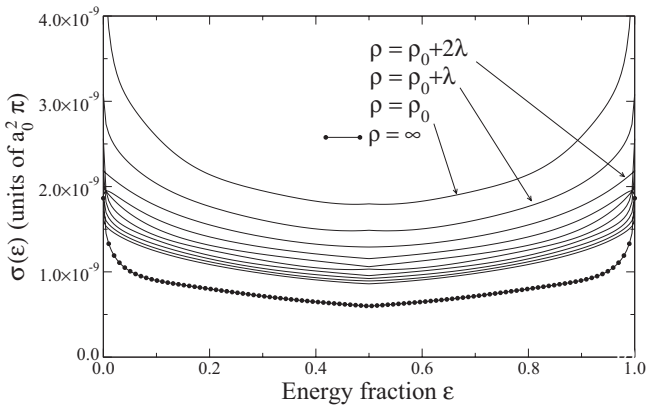

FIG. 5. Single differential cross section for the S-wave model $(e,3e)$ process for $q = 0.24$ a.u. The equal energy fraction value corresponds to ionized electron energies equal to 10 eV. Continuous line: SDCS evaluated with the flux formula for different values of $\rho_n = \rho_0 + n\lambda$ ($\lambda = \frac{2\pi}{\sqrt{2E}}$, $\rho_0 = 2\lambda$). Circles: $\rho \to \infty$ extrapolated results.

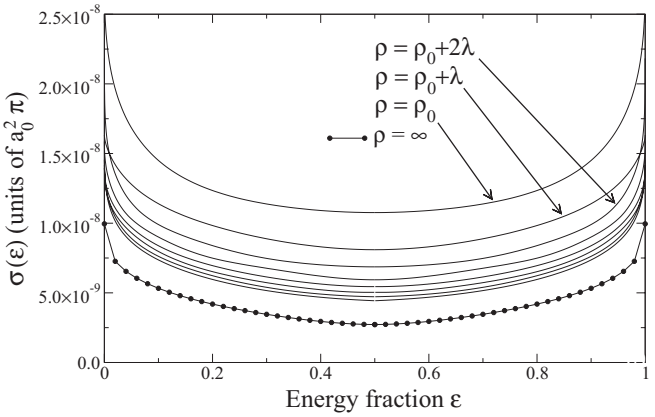

FIG. 6. Single differential cross section for the S-wave model $(e,3e)$ process for $q = 0.22$ a.u. The equal energy fraction value corresponds to ionized electron energies equal to 4 eV. Continuous line: SDCS evaluated with the flux formula for different values of $\rho_n = \rho_0 + n\lambda$ ($\lambda = \frac{2\pi}{\sqrt{2E}}$, $\rho_0 = 2\lambda$). Circles: $\rho \to \infty$ extrapolated results.

TABLE I. Single differential cross section for the $(e,3e)$ process at an impact energy $E_i = 5599$ eV and momentum $k_i = 20.29$ a.u. First column: energy fraction of the "slow" two-electron system. Second column: SDCS for the case where the "slow" two-electron system energy is $E = 0.294$ a.u. (process where the case $4+4$ eV electrons can be found); this corresponds to a final projectile momentum $k_f = 20.13$ a.u. and momentum transfer $q = 0.22$ a.u. Third column: same as the second column but for the final state compatible with the $10+10$ eV electrons final state, where $E = 0.735$ a.u., $k_f = 20.11$ a.u., and $q = 0.24$ a.u.

	SDCS $\times 10^{-9}$	
ε/E	$q = 0.22$ a.u. $(4+4$ case)	$q = 0.24$ a.u. $(10+10$ case)
0.0	1.863 74	2.759 63
0.025	1.147 27	2.119 05
0.05	1.009 17	1.954 15
0.075	0.940 59	1.838 50
0.1	0.899 47	1.743 66
0.125	0.870 16	1.661 13
0.15	0.845 63	1.587 47
0.175	0.822 76	1.520 93
0.2	0.800 37	1.460 39
0.225	0.778 22	1.404 88
0.25	0.756 49	1.353 56
0.275	0.735 51	1.305 62
0.3	0.715 55	1.260 20
0.325	0.696 80	1.216 43
0.35	0.679 34	1.173 46
0.375	0.663 17	1.130 38
0.4	0.648 22	1.086 31
0.425	0.634 37	1.040 34
0.45	0.621 49	0.991 56
0.475	0.609 45	0.939 11
0.5	0.598 13	0.894 05

a direct comparison cannot be presented since, in these references, the SDCS result from considering a situation where all three electrons share the energy of the system. This differs from the Orsay experiment in which the incident electron is

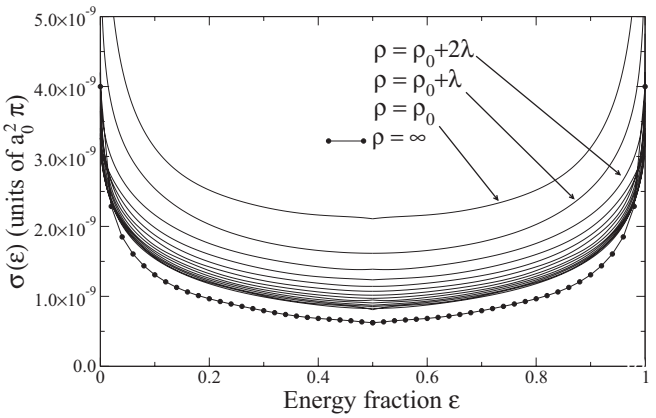

FIG. 7. Single differential cross section for the *S*-wave model $(e,3e)$ process for $q = 0.635$ a.u. The equal energy fraction value corresponds to ionized electron energies equal to 10 eV. Continuous line: SDCS evaluated with the flux formula for different values of $\rho_n = \rho_0 + n\lambda$ $(\lambda = \frac{2\pi}{\sqrt{2E}},\ \rho_0 = 2\lambda)$. Circles: $\rho \to \infty$ extrapolated results.

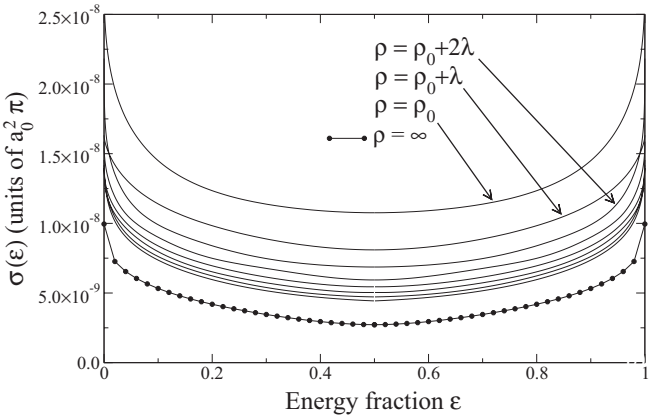

FIG. 8. Single differential cross section for the *S*-wave model $(e,3e)$ process for $q = 0.555$ a.u. The equal energy fraction value corresponds to ionized electron energies equal to 4 eV. Continuous line: SDCS evaluated with the flux formula for different values of $\rho_n = \rho_0 + n\lambda$ $(\lambda = \frac{2\pi}{\sqrt{2E}},\ \rho_0 = 2\lambda)$. Circles: $\rho \to \infty$ extrapolated results.

scattered with a given fixed energy. This said, we have also considered the case of an incident energy of 500 eV, still scattered at the same small scattering angle (0.45°) of the Orsay experiments; the two ejected electrons escape with $10+10$ eV or $4+4$ eV, corresponding to $q = 0.635$ a.u. and $q = 0.555$ a.u., respectively. Following the same calculation procedure, the resulting SDCS (presented in Figs. 7 and 8) have shapes

TABLE II. Same as Table I but for an incident electron energy and momentum equal to 500 eV and $k_i = 6.06$ a.u., respectively. In this case the second column $(4+4$ eV) is associated to the following kinematics: $E = 0.294$ a.u., $k_f = 5.43$ a.u., and $q = 0.635$ a.u. For the third column $(10+10$ eV) corresponds to $E = 0.735$ a.u., $k_f = 5.51$ a.u., and $q = 0.55$ a.u.

	SDCS $\times 10^{-9}$	
ε/E	$q = 0.55$ a.u.$(4+4$ case)	$q = 0.635$ a.u. $(10+10$ case)
0.0	9.95	4.00
0.025	7.08	2.18
0.05	6.29	1.73
0.075	5.75	1.48
0.1	5.33	1.31
0.125	4.98	1.19
0.15	4.69	1.10
0.175	4.42	1.02
0.2	4.19	0.97
0.225	3.99	0.92
0.25	3.80	0.87
0.275	3.62	0.83
0.3	3.46	0.79
0.325	3.31	0.76
0.35	3.18	0.73
0.375	3.05	0.70
0.4	2.95	0.68
0.425	2.86	0.67
0.45	2.79	0.66
0.475	2.74	0.64
0.5	2.72	0.62

similar to those corresponding to the higher impact energy of 5599 eV, but have larger magnitudes (see Table II). The 500 eV case could be of interest for elucidating the limit at which the Born approximation starts to be valid. Comparing our three-body results with those coming out of a full four-body calculation could indicate whether or not agreement is found already at this relatively low incident energy.

IV. CONCLUDING REMARKS

In this paper we presented an original transformation of the four-body Schrödinger equation for high-energy-electron-impact double ionization of helium. Successive orders in the projectile-target interaction appear in a set of driven equations. From the asymptotic form of the first-order solution the corresponding transition amplitude is shown to be equivalent to the first Born approximation used in most publications.

As several *ab initio* three-body methods do not agree with each other for high-energy $(e,3e)$ processes, we looked for a simplified problem for which agreement could possibly be found. We thus considered an S-wave $(e,3e)$ model with energy and geometry conditions used by the experimental Orsay group. Our three-body model differs from the one investigated in Refs. [27,28], where the full four-body problem was considered. In our case we deal with a three-body problem which results when high-energy projectiles are considered; besides, contrary to the study of [27,28], our calculated cross sections correspond to the sharing between two ejected electrons of a given energy. We have also considered a lower impact energy (500 eV) to make a connection with nonperturbative methods; our cross sections could serve as a test of the range of validity of the first Born approximation. The first-order driven equation was solved numerically with a generalized Sturmian approach; two independent numerical implementations (spherical and hyperspherical) were shown to be in excellent agreement. From the asymptotic form of our *ab initio* solution we extracted the transition amplitude and calculated single differential cross sections. We hope that the present results will be of value to others and that they will stimulate other *ab initio* calculations. If agreement can be found for the present model, one would then attribute the existing differences for the real $(e,3e)$ process to $L \neq 0$ and/or convergence issues.

ACKNOWLEDGMENTS

This work has been developed within the activities planned in the French-Argentinian program ECOS-Sud A10E01. The support by ANPCyT (PICT08/0934) (Argentina) and PIP 200901/552 CONICET (Argentina) is acknowledged. G.G. also thanks the support by PGI (24/F049) of the Universidad Nacional del Sur.

[1] A. Lahmam-Bennani, I. Taouil, A. Duguet, M. Lecas, L. Avaldi, and J. Berakdar, Phys. Rev. A **59**, 3548 (1999).
[2] A. Kheifets, I. Bray, A. Lahmam-Bennani, A. Duguet, and I. Taouil, J. Phys. B **32**, 5047 (1999).
[3] L. U. Ancarani, C. Dal Cappello, and G. Gasaneo, J. Phys.: Conf. Ser. **212**, 012025 (2010).
[4] J. Berakdar, A. Lahmam-Bennani, and C. Dal Cappello, Phys. Rep. **374**, 91 (2003).
[5] M. S. Pindzola *et al.*, J. Phys. B **40**, R39 (2007).
[6] V. A. Knyr, V. V. Nasyrov, and Yu. V. Popov, in *Correlation and Polarization in Photonic, Electronic, and Atomic Collisions*, edited by G. F. Hanne *et al.*, AIP Conf. Proc. No. 697 (AIP, Melville, NY, 2003), p. 76.
[7] S. A. Zaytsev, V. A. Knyr, and Yu. V. Popov, Phys. At. Nucl. **70**, 676 (2007).
[8] I. Bray, J. Phys. B **36**, 2203 (2003).
[9] C. W. McCurdy, M. Baertschy, and T. N. Rescigno, J. Phys. B **37**, R137 (2004).
[10] M. S. Pindzola, F. Robicheaux, and J. Colgan, J. Phys. B **41**, 235202 (2008).
[11] M. S. Pindzola, Sh. A. Abdel-Naby, J. Colgan, and A. Dorn, J. Phys. B **45**, 215208 (2012).
[12] V. V. Serov, V. L. Derbov, B. B. Joulakian, and S. I. Vinitsky, Phys. Rev. A **75**, 012715 (2007).
[13] A. S. Kheifets and I. Bray, Phys. Rev. A **69**, 050701(R) (2004).
[14] M. S. Mengoue, M. G. K. Njock, B. Piraux, Y. V. Popov, and S. A. Zaytsev, Phys. Rev. A **83**, 052708 (2011).
[15] A. L. Frapiccini, J. M. Randazzo, G. Gasaneo, and F. D. Colavecchia, J. Phys. B **43**, 101001 (2010).
[16] J. M. Randazzo, F. Buezas, A. L. Frapiccini, F. D. Colavecchia, and G. Gasaneo, Phys. Rev. A **84**, 052715 (2011).
[17] D. M. Mitnik, F. D. Colavecchia, G. Gasaneo, and J. M. Randazzo, Comput. Phys. Commun. **182**, 1145 (2011).
[18] G. Gasaneo, D. M. Mitnik, J. M. Randazzo, A. L. Frapiccini, and F. D. Colavecchia, J. Phys. Chem. A **113**, 14573 (2010).
[19] G. Gasaneo and L. U. Ancarani, J. Phys. A **45**, 045304 (2012).
[20] A. Temkin, Phys. Rev. **126**, 130 (1962).
[21] R. Poet, J. Phys. B **11**, 3081 (1978).
[22] L. U. Ancarani, G. Gasaneo, and D. M. Mitnik, Eur. Phys. J. D **66**, 270 (2012).
[23] D. M. Mitnik, G. Gasaneo, and L. U. Ancarani, J. Phys. B **46**, 015202 (2013).
[24] M. S. Pindzola, D. Mitnik, and F. Robicheaux, Phys. Rev. A **59**, 4390 (1999).
[25] C. Plottke, I. Bray, D. V. Fursa, and A. T. Stelbovics, Phys. Rev. A **65**, 032701 (2002).
[26] D. A. Horner, C. W. McCurdy, and T. N. Rescigno, Phys. Rev. A **71**, 012701 (2005).
[27] P. L. Bartlett and A. T. Stelbovics, Phys. Rev. A **81**, 022715 (2010).
[28] P. L. Bartlett and A. T. Stelbovics, Phys. Rev. A **81**, 022716 (2010).
[29] D. A. Konovalov, D. V. Fursa, and I. Bray, Phys. Rev. A **84**, 032707 (2011).
[30] S. Elazzouzi, C. Dal Cappello, A. Lahmam-Bennani, and F. Catoire, J. Phys. B **38**, 1391 (2005).

[31] C. J. Joachain, *Quantum Collision Theory* (North-Holland, Amsterdam, 1983).
[32] A. S. Kadyrov, A. M. Mukhamedzhanov, A. T. Stelbovics, I. Bray, and F. Pirlepesov, Phys. Rev. A **68**, 022703 (2003).
[33] E. O. Alt and A. M. Mukhamedzhanov, Phys. Rev. A **47**, 2004 (1993).
[34] S. D. López, C. R. Garibotti, and S. Otranto, Phys. Rev. A **83**, 062702 (2011).
[35] M. J. Ambrosio, J. A. Del Punta, K. V. Rodriguez, G. Gasaneo, and L. U. Ancarani, J. Phys. A **45**, 015201 (2012).
[36] J. M. Randazzo, A. L. Frapiccini, F. D. Colavecchia, and G. Gasaneo, Phys. Rev. A **79**, 022507 (2009).
[37] J. M. Randazzo, L. U. Ancarani, G. Gasaneo, A. L. Frapiccini, and F. D. Colavecchia, Phys. Rev. A **81**, 042520 (2010).
[38] C. W. McCurdy and T. N. Rescigno, Phys. Rev. A **62**, 032712 (2000).
[39] R. K. Peterkop, *Theory of Ionization of Atoms by Electron Impact* (Colorado Associated University Press, Boulder, CO, 1977).
[40] M. Baertschy, T. N. Rescigno, W. A. Isaacs, and C. W. McCurdy, Phys. Rev. A **60**, R13 (1999).
[41] J. M. Randazzo *et al.* (unpublished) (2012).
[42] C. W. McCurdy and T. N. Rescigno, Phys. Rev. A **56**, R4369 (1997).